



# HHS Public Access

Author manuscript

*Biomed Signal Process Control*. Author manuscript; available in PMC 2017 January 01.

Published in final edited form as:

*Biomed Signal Process Control*. 2016 January ; 23: 76–84. doi:10.1016/j.bspc.2015.07.008.

## Current Source Mapping by Spontaneous MEG and ECoG in Piglets Model

Lin Gao<sup>a</sup>, Jue Wang<sup>a,1</sup>, Julia Stephen<sup>b</sup>, and Tongsheng Zhang<sup>c</sup>

<sup>a</sup>Institute of Biomedical Engineering, Key Laboratory of Biomedical Information Engineering of Education Ministry, Xi'an Jiaotong University, Xi'an 710049, Shaanxi, P. R. China

<sup>b</sup>The Mind Research Network, Albuquerque, NM 87131, USA

<sup>c</sup>Department of Neurology, University of New Mexico, Albuquerque, NM 87131, USA

### Abstract

The previous research reveals the presence of relatively strong spatial correlations from spontaneous activity over cortex in Electroencephalography (EEG) and Magnetoencephalography (MEG) measurement. A critical obstacle in MEG current source mapping is that strong background activity masks the relatively weak local information. In this paper, the hypothesis is that the dominant components of this background activity can be captured by the first Principal Component (PC) after employing Principal Component Analysis (PCA), thus discarding the first PC before the back projection would enhance the exposure of the information carried by a subset of sensors that reflects the local neuronal activity. By detecting MEG signals densely (one measurement per  $2 \times 2 \text{ mm}^2$ ) in three piglets neocortical models over an area of  $18 \times 26 \text{ mm}^2$  with a special shape of lesion by means of a  $\mu\text{SQUID}$ , this basic idea was demonstrated by the fact that a strong activity could be imaged in the lesion region after removing the first PC in Delta, Theta and Alpha band, while the original recordings did not show such activity clearly. Thus, the PCA decomposition can be employed to expose the local activity, which is around the lesion in the piglets' neocortical models, by removing the dominant components of the background activity.

### Keywords

Principle Component Analysis; Background Activity; Lesion; Piglet Neocortical Model; MEG

### 1. Introduction

Magnetoencephalography (MEG) measures the weak magnetic field produced by small current flow in the brain. MEG signals can be transformed to obtain a first-order estimate of coherent current flow below a 4-channel superconducting quantum interference device (SQUID) array [1]. Cohen et al. has shown originally that the outputs from two orthogonally oriented pairs of planar gradiometer detectors can be used to measure the magnitude and direction of the current located below the center of such a detector [1]. The two pairs of gradiometers can be emulated by the microSQUID ( $\mu\text{SQUID}$ ), by combining the outputs

<sup>1</sup>Corresponding author: juewang@mail.xjtu.edu.cn.

from an orthogonal pair to measure the gradient of  $B_z$  along the  $x$ -axis,  $B_z/\Delta x$ , and by combining the outputs from the other pair to measure  $B_z/\Delta y$ . Both of these gradients are maximum below the center of the detector array. It can be shown that both the magnitude and phase of the current vector at the center of the detector array can be correctly estimated to a scale factor. Therefore, the magnitude  $I$  of a current is given as

$$I = \frac{4\pi R^3}{\mu_0 d} \sqrt{\left(\frac{\Delta B_z}{\Delta x}\right)^2 + \left(\frac{\Delta B_z}{\Delta y}\right)^2} \quad (1)$$

Where  $R$  is the distance from the current vector to each coil,  $d$  is the separation between the diagonally opposite sensors and  $\mu_0$  is the permeability of free space. The phase  $\phi$  is given by

$$\arctan\left(\frac{\Delta B_z/\Delta x}{\Delta B_z/\Delta y}\right) \quad (2)$$

Cohen et al. believed this model could be applied for the dc current imaging that produces the dc magnetic field in entire human body [1]. Henceforward, this model for detecting the current source beneath its center is believed to establish a base for imaging cortex activity magnetically. If every coil contains only the local information, then the gradient should reflect the center current flow beneath the two coils.

However, real cortex is far from the dc current model as above. Due to the distance from the sources, a coil could never reflect only the local information. In particular, there are many random sources firing simultaneously in the cortex. The non-stationarity of EEG and MEG is well documented [2]. Thus, the approach above needs improvement for current localization in cerebral cortex with MEG.

The strong spatial correlation across the recording sites was reported in MEG data [3–5]. The previous work already learnt that spontaneous MEG measurement from pig cortex detected by our 4-coil SQUID system was highly correlated [6]. The generation of such activity is not clear. It is perhaps caused by spontaneous potential or the sufficient external noise. The lead field of 4-coil SQUID is believed to produce high correlation. Besides that, there are bleed across the measurement area, which may be also one reason for the correlation. Based on the analysis above, the high correlation could be hardly related to local tissues. This correlated activity occurred over the whole cortex making it difficult to specify local activity. Therefore, that removal of the highly spatially correlated components might be better to reveal local activity.

When preprocessing multi-channel data, Principle Component Analysis (PCA) is usually used as a denoising approach to improve the signal to noise ratio (SNR) by keeping the first few PCs while discarding the residuals [7]. An opposite use of the PCA, namely Principal Component Elimination Method (PCEM), was previously proposed to remove the spontaneous MEG, which is considered as noise in the analysis of evoked data, and enhance

the SNR for evoked MEG measurement by eliminating the 1st PC [8]. In this paper, spontaneous MEG over the piglets' neocortex was scanned by a 4-channel  $\mu$ SQUID array with two orthogonally oriented pairs of planar gradiometer detectors in the recording plane of about 18 mm by 26 mm with 2 mm step. It is hypothesized that the activity around the border of the lesion in the neocortex was strong local activity, which was orthogonal to the background recordings. Based on such a hypothesis, the utility of PCA preprocessing was investigated in animal MEG recordings at revealing local activity after the background activity has been removed. Because MEG and EEG share many similar characteristics and are often analyzed using the same methods and tools, the results should be applied broadly to both MEG and EEG.

## 2. Materials and methods

### 2.1. Methods

**2.1.1. Normalized Principal Component Analysis**—In our study, the multi-channel signal model at a time point is described by Eq. (3).

$$S = S_{spont} + S_{lesion} + S_{external} + S_n \quad (3)$$

Where the multi-dimensional data detected by the MEG system are composed of 4 components. They are the on-going spontaneous activity  $S_{spont}$ , the lesion activity  $S_{lesion}$ , the external interferences  $S_{external}$  and the normally distributed white noise  $S_n$ . The first step in our data analysis procedure is to normalize the amplitude from each channel by its own standard deviation (SD) to set the same weight for all sensors before applying PCA decomposition, as expressed by Eq. (4).

$$\bar{S} = S / SD \quad (4)$$

$\bar{S}$  is the normalized recording based on each channel's  $SD$ . The PCA decomposition could be applied after filtering. The transformation is defined by a set of 4-dimensional vectors of weights or loadings  $w_{(4)} = (w_1, \dots, w_4)_{(k)}$  that map each vector  $\bar{S}_{(i)}$  of  $\bar{S}$  to a new vector of principle component scores  $t_{(i)} = (t_1, \dots, t_4)_{(i)}$ , given by

$$t_{k(i)} = \bar{S}_{(i)} \cdot w_{(k)} \quad (5)$$

The individual variables of  $t$  considered inherit the maximum variance from  $\bar{S}$ . The first loading vector  $w_{(1)}$  has to satisfy

$$w_{(1)} = \arg \max_{\|w\|=1} \left\{ \sum_i (t_1)_{(i)}^2 \right\} \quad (6)$$

The first PC can then be defined as the corresponding vector in the original variables  $\{\bar{S}_{(j)} \cdot w_{(1)}\}$ . In this paper, there are only 4 channels for MEG measurement, and the hypothesis is that the first PC represents the dominant component of background activity. The largest PC also captures external interference  $S_{external}$  since interference from distant sources appears more or less in all channels. Local activity carried by relatively a few channels is the interested activity in our study. The normalization is a very important step to avoid a special situation where a few channels with very strong magnitude in our model are recognized as the major PC; this ensures that only the globally distributed temporal patterns in the data can be represented by the first PC. Here, globally indicates all or most of the channels in the sensor array.

After discarding the back projection of the largest PC, the background activity across sensors is reduced, and the residual is named as  $\overline{S_{res}}$ , as represented by Eq. (7).

$$\overline{S_{res}} = S_{spont\_res} + S_{lesion} + S_{external\_res} + S_n \quad (7)$$

Wherein  $S_{spont\_res}$  and  $S_{external\_res}$  are the retained residuals after discarding the largest PCs.

**2.1.2. Local information ratio**—In our study, local information ratio is defined as the ratio of the average SD in the lesion region over that in the rest of the scanning area for each channel:

$$r = \frac{ave\_SD_{lesion}}{ave\_SD_{rest}} \quad (8)$$

Wherein  $r$  represents local information ratio,  $ave\_SD_{lesion}$  is the average SD over the lesion area, and  $ave\_SD_{rest}$  is the average SD in the rest area. The  $ave\_SD_{rest}$  stands for the background activity, while the  $ave\_SD_{lesion}$  represents the local activity, which is around the lesion in our paper. The rest region was obtained by subtracting lesion area from the scanning region here.

The data were processed by Matlab software in our study.

## 2.2. Animal experiments

Three juvenile farm pigs (*Sus scrofa*, 3–5 weeks old, 7–12 kg) were studied while maintaining the animals in stable condition. Animals were prepared as previously described [9–11] using a protocol approved by the University of New Mexico School of Medicine and Albuquerque VA Medical Center. The piglets were initially sedated with 1% thiopental

sodium (25 mg/kg, i.t.) or with a combination of ketamine (16 mg/kg, i.m.) and xylazine (4 mg/kg, i.m.) in the animal facility, and were transported to the operating room. The animals were then anesthetized intravenously with sodium thiopental (9 mg/kg/h), artificially ventilated and secured in a custom-made head holder using paramagnetic materials (copper and flex glass). Additional anesthetics were given as needed to maintain a surgical level of anesthesia. The scalp and skull were removed and the right hemisphere was turned up to face the sensors of the MEG system called  $\mu$ SQUID designed specifically for in vivo and in vitro studies [10]. Barbiturate anesthesia was reduced to 3 mg/kg/h in order to achieve a light anesthetic level corresponding to stage I/II sleep level. The sleep level was continuously monitored with ECoG (Electrocorticography). Tubocurarine chloride was given 0.3 mg/kg/h intravenously to prevent reflexive movements. The electrocardiogram was monitored continuously to ascertain sufficient anesthetic levels. Blood gas was monitored to check for adequacy of ventilation.

The  $\mu$ SQUID was housed in a magnetically shielded room. It is equipped with four first-order, symmetric channels of the magnetometers with 4.0 mm diameter pickup coils, 8.5 mm diagonal separation between channels, 16 mm baseline, 1.2 mm separation between the detection coils and the outside surface of the cryogenic container of the  $\mu$ SQUID with a noise level of  $50 fT/\sqrt{Hz}$ , with an exception that one channel (channel 1) has a higher noise level ( $80 fT/\sqrt{Hz}$ ). The four-channel configuration in the  $\mu$ SQUID is schematically illustrated in Fig. 1(a) and Fig. 1(b). The SQUID outputs were fed to a 4-channel amplifier with a 24 db/octave Butterworth filter. All magnetic field data were collected with a bandpass filter with a high- and low-pass cut-off frequency of 0.1 Hz and 1 KHz, respectively. Constrained by the configuration of the  $\mu$ SQUID, the neocortical area of interest cannot be fully covered with simultaneous recordings; therefore, the area of interest was scanned by moving the animal platform relative to the  $\mu$ SQUID at steps of 2 mm as in Fig. 1(a). At each scan location, 16 seconds of data were recorded. Prior to making a lesion, a baseline measurement was carried out by scanning the  $\mu$ SQUID over a predetermined, relatively flat region of primary somatosensory cortex (SI) by recording the normal spontaneous brain activity. Our strategy was to create a lesion surgically with non-active tissue in close proximity to active background neuronal sources. The lesion was ablated by sucking off a special shape of neocortex and then filled with biocompatible material (3% agar prepared with saline solution). The location of the lesion measuring  $\sim 6$  mm in diameter was chosen by avoiding the visually sizable arterials as in Fig. 1(a), in order to reduce the damage to the surrounding brain. Along with the MEG detectors, 28 channels of ECoG, centered on the lesion, over the predetermined flat cortical region were simultaneously recorded (Fig. 1(c)). The ECoG electrode pat was custom-made by weaving silver wires (125 micrometer in diameter, coated with Teflon) with a thin nylon net sheet. The active tips of the electrodes were silver-silver chloride. After a multichannel pre-amplifier (customarily made to be compatible with biomagnetic signal detection in the  $\mu$ SQUID magnetically shielded room) with 5x amplification, ECoG signals were fed to a signal conditioner (SCXI-1000, National Instruments) for anti-aliasing filtering. MEG and ECoG were sampled at 2048 Hz using self-made data collection software developed in Labview (National Instruments). ECoG is usually taken as a gold standard to describe the neocortical neuronal

activation [12]. The ECoG recordings were used as a reference to analyze the simultaneously recorded MEG signals.

Spontaneous MEG over the neocortex was scanned by the  $\mu$ SQUID in the recording plane of about 18 mm by 26 mm with 2 mm step (Fig. 1(a)). The recording plane was 5.5 mm above the cortex. Three replications of 16 seconds MEG with sampling frequency of 2048Hz were recorded consecutively to check reliability of mapping for each piglet. As mentioned above, ECoG was also recorded in the neo-cortex of the piglets by 28 silver chloride electrodes with 5 mm space, as shown in Fig. 1(c).

Spontaneous activity from the pig cortex detected by the 4-coil  $\mu$ SQUID system was strongly correlated [6]. In order to prove that PCA processing can remove overall background activity and thus expose the local information, PCA was applied to de-correlate the 4 channels and to locate the inactive area of the cerebral cortex. The activity in Delta band (0.1–5 Hz) is a sign of neurological damage [13–15], therefore the effect of PCA decomposition was studied on the separation of local and global background activity in the Delta frequency band. Additionally, the effect of PCA removal was also explored in main physiological frequency bands including: Theta (5–8 Hz), and Alpha (8–13 Hz) band. The SD matrix of the recorded MEG before and after applying our preprocessing procedure at each detection site over the scanned area was imaged to investigate the magnetic field distribution.

### 3. Results

Fig. 2(a) reveals the location of three selected electrodes, where 3 individual electrodes are located in the lesion, at the edge of the lesion, and at an intact neocortical area which is about 18 mm far away from the edge of the lesion. Fig. 2(b) shows 10 seconds ECoG signals, among them the spontaneous signal from the intact neocortex region has an SD that is 3 times smaller than the signal coming from the electrode at the border of the lesion (periphery), while the electrode in the lesion (agar) did not detect any noticeable signals. The frequency spectrum of the ECoG signals at the periphery and the intact area was generated via a Fourier transform of the signal, and the resulting value was usually presented as power plotted versus frequency. The corresponding spectrum of the two electrodes was plotted in Fig. 2(c). Note that the spectrum for the electrode in the lesion was not shown due to the obvious zero value in Fig. 2(b). The gold standard, ECoG data, showed strong Delta activity (0.1–5 Hz) at the border of the lesion illustrated by Fig. 2. Additionally, the activities at Theta (5–8 Hz) and Alpha (8–13 Hz) band were also stronger than the intact area, but relatively weaker than Delta activity.

The SD value imaging calculated from ECoG signal was plotted to provide the evidence for the existence of inactivity area in Fig. 3. It demonstrated that the lesion area generated weak activity, while the strong activity was produced by the periphery. Although the measurement scope in ECoG was not completely the same as in MEG, it still shows the animal model was established with strong activity in the lesion periphery.

Fig. 4(a) shows a typical 1-second long spontaneous MEG signal recorded over SI region by the 4-channel  $\mu$ SQUID. A common pattern in the background dominated the recordings and was spatially correlated in sensor space. A PCA analysis of the signal shown in Fig. 4(a) is illustrated in Fig. 4(b) from PC 1 to 4, respectively, which demonstrates that the PC1 represents the largest variance of the recordings with a percentage of 57.93%. After projecting the first PC back to the measurement space, i.e. the 4 channels of the  $\mu$ SQUID, it can be clearly seen the strongly correlated background signals characterized with the same dynamic pattern as in the original signal over all channels, as depicted in Fig. 4(c). The correlation coefficients between Fig. 4(a) and Fig. 4(c) are 0.9433, 0.6583, 0.6281, and 0.7748 for each channel respectively, which quantitatively validate the claim that they indeed share 'the same dynamic pattern'.

As shown above, the 1<sup>st</sup> PC has the largest variance. The study then concentrated on the signals back projected from the remaining 3 PCs, and compared with the original recordings to determine if local activity could be better identified. Channel 2 was used to indicate the results by imaging the SD value in Delta, Theta and Alpha frequency band. Fig. 5(a) indicates an ideal model pattern of SD imaging for Channel 2. In the left three plots in Fig. 5 (Fig. 5(b), Fig. 5(e) and Fig. 5(h)), the SD value of the original coil 2 was shown in the Delta (0.1–5 Hz), Theta (5–8 Hz), and Alpha (8–13 Hz) frequency band respectively. Fig. 5(b) demonstrates that a neocortical lesion filled with agar is a reasonable model to generate local strong Delta activity compared with the large neocortical surface, while the activity in Theta and Alpha band could not be recognized in Fig. 5(e) and Fig. 5(h). Due to the strong Delta wave generated at the margin of the lesion, resolution of the MEG measurement cannot distinguish the margin from the lesion itself compared with the image of ECoG recordings in Fig. 3. The SD value of the PC1 projection to coil 2 in the same frequency band is plotted in the middle plots in Fig. 5, while SD value of the reconstruction by back projection of PC2, PC3, and PC4, i.e., the residuals, is in the right plottings in Fig. 5 in the Delta (0.1–5 Hz), Theta (5–8 Hz), and Alpha (8–13 Hz) frequency band respectively. In the Delta band, Fig. 5(c) demonstrates the lesion with strong Delta activity, which is similar to Fig. 5(b), while Fig. 5(d) shows a faint inactive spot in the corresponding area. As to Theta and Alpha frequency band, interestingly, a lesion opening with strong activity can also be ambiguously seen in Fig. 5(f) and Fig. 5(i) after PCA preprocessing, while weak activity can be seen faintly in the lesion region in Fig. 5(g) and Fig. 5(j), although other three coils always left hot spots around the lesion.

Again, Channel 2 was employed to demonstrate the results by imaging the SD value at Delta, Theta and Alpha band, after normalizing each channel at each recording site prior to the PCA decomposition (see the left three plots in Fig. 6, i.e. Fig. 6(a), Fig. 6(d) and Fig. 6(g)). The middle three plots in Fig. 6 (Fig. 6(b), Fig. 6(e), and Fig. 6(h)) illustrate the SD value of the PC1 projection to coil 2 in the same frequency band, while SD value of the reconstruction by back projection of the residuals, is plotted in right three plots in Fig. 6 (Fig. 6(c), Fig. 6(f), and Fig. 6(i)) corresponding to Delta, Theta and Alpha band. As expected, the lesion is not as visible for the original data with normalization (Fig. 6(a), Fig. 6(d) and Fig. 6(g)). Compared with the imaging without normalization in Fig. 5(b) in Delta band, the original image as shown in Fig. 6(a) faintly shows a relative stronger activity at the center, but is associated with several other hot spots. That is, the strong local activity is no

longer dominant with normalization. The images of the 1<sup>st</sup> PC projection, as shown in Fig. 6(b), Fig. 6(e) and Fig. 6(h), clearly demonstrate that there is a lack of background activity in the lesion, which was filled with foreign materials, i.e., agar in our studies. The comparison between lesion and background activity in Delta band (Fig. 6(b)) is obviously stronger than in Theta band (Fig. 6(e)) and Alpha band (Fig. 6(h)). In contrast, Fig. 6(c), Fig. 6(f), Fig. 6(i) indicate a strong local activity in the lesion area, although the lesion activity in Theta (Fig. 6(f)) and Alpha band (Fig. 6(i)) is not so clear as in Delta band (Fig. 6(c)). Fig. 6 demonstrates that the global (Fig. 6(b), Fig. 6(e) and Fig. 6(h)) and local (Fig. 6(c), Fig. 6(f) and Fig. 6(i)) information is clearly separated by the normalized PCA, which poses a contrast with PCA without normalization in Fig. 5. Fig. 6 demonstrates that PCA decomposition after normalization retains the large amplitude, but spatially limited signal. Consistent results, not shown here, were obtained for the other three coils.

The effect of normalized PCA on the MEG signals was explored. The time series of MEG signals in the intact area and lesion area were selected respectively as in Fig. 7(a), and the frequency spectrum of the original signal after normalization, the first PC, and the residuals after discarding the first PC was calculated in Fig. 7(b) to Fig. 7(d) for the signal in the lesion, and in Fig. 7(e) to Fig. 7(g) for the signal in the intact area. Fig. 7(b) reveals rather strong Delta activity in the lesion area for the original data after normalization, while Fig. 7(e) indicates activity in Delta, Theta and Alpha band. After PCA preprocessing, the strong Delta activity was retained in the residuals for the signal in the lesion as in Fig. 7(d), while the PC1 contains mostly the very weak activity in 0.1 Hz to 10 Hz as in Fig. 7(c), which demonstrates that the activity in the lesion could not represent the global activity, and the first PC could hardly captures its activity. In contrast, the first PC represents most activities for the signal in the intact area in physiological frequency bands (Fig. 7(f)) compared with the residuals (Fig. 7(g)). That's why the first PC reveals strong activity in the background and the relative weak activity in the lesion area, while the residues show opposite phenomenon.

The same procedure of SD imaging without and with normalized PCA preprocessing was performed in three piglets. The images of other two piglets, not shown here, indicate the consistent pattern, although the lesion areas are not all centered. Fig. 8 demonstrates the average local information ratio over four channels with and without normalized PCA for three piglets, i.e. the average local information ratio for original data and the residuals after normalization, in Delta (0.1–5 Hz), Theta (5–8 Hz), and Alpha (8–13 Hz) band. The results demonstrate that the average local information ratio with preprocessing is larger than the ratio for original data. A t-test was performed on average local information ratio with and without normalized PCA preprocessing across the 3 piglets here in different frequency bands respectively. A null hypothesis is that the average local information ratio with and without preprocessing comes from distributions with equal means. The results demonstrate the hypothesis can be rejected at 5% level in all the frequency bands, which statistically proves the effect of normalized PCA on enhancing local information ratio across three piglets.

## 4. Discussions and conclusions

In multichannel recordings, PCA is usually used to improve the SNR by discarding the smaller PCs. In this paper, the PCA was applied opposite to the convention such that the largest PC was discarded while the smaller PCs remained. It must be emphasized that our approach does not aim at improving the overall SNR, but on increasing the local information ratio.

Because of the external noise, the field effect spread to the sensors caused by the large distance between the magnetometer coils and the sources, and the ubiquitous spontaneous potential over cortex, MEG yields relatively large extracranial coherence even when the underlying brain sources are uncorrelated [16,17]. In addition, each MEG coil is sensitive to a large region of the cortex [18]. Therefore, the background activity results from the external noise, the field effect between coils and cortex, the overlap of the sensitivity area of different coils, and the spontaneous potential. The PCA decomposition is already known for the improvement of SNR for evoked responses, prior to averaging, by eliminating the influence of the spontaneous potential [8]. For this research, initially an animal model was used to well define the activity around the lesion as local activity. Then this lesion activity was separated from the background activity by removing the first PC from recordings taken, which confirmed our basic idea that the local information can be enhanced by discarding the first PC in a multichannel MEG recording system. The frequency spectrum of first PC after normalized PCA in Fig. 7 indicates that the removed PC mainly falls into physiological frequency bands, which proves that the normalization PCA here is not a preprocessing approach to remove the noise and enhance the SNR, but focus on the separation of local activity from global activity mainly resulting from spontaneous activity.

In this study, the SD imaging results of animal data with normalized PCA decomposition preprocessing demonstrated that the first PC mainly contained the overall correlated components of the MEG recordings, and that the local information was enhanced by keeping the rest of the PCs. After removing the first PC, each coil kept enough “local” information in order to image the underlying sources. Fig. 5(b) shows that there was strong activity in the lesion region and the activity was, apparently, locally distributed in Delta band, while there is no distinguishable activity in Theta and Alpha band in Fig. 5(e) and Fig. 5(h). After PCA preprocessing without normalization, the lesion activity could almost be recognized, although it is ambiguous and greatly influenced by other channels. After applying the normalized PCA, the first PC representing the activity in the background, clearly illustrated a weak activity in the lesion area that was different from the intact neocortex, as shown in Fig. 6(b) in Delta band, Fig. 6(e) in Theta band, and Fig. 6(h) in Alpha band, while the local activity in the lesion area was well captured by the residuals after removing the 1st PC in Fig. 6(c), Fig. 6(f) and Fig. 6(i) correspondingly. Thus, it could be inferred that the average local information ratio could be improved by the normalized PCA as in Fig. 8. The consistent pattern was obtained in three piglets.

Delta band activity is regarded as a marker to reflect structural damage, e.g., cerebral infarct, contusion, local infection, tumor, subdural hematoma, mild cognitive impairment, aphasia, dyslexia, schizophrenia or depression [13–15]. Nagata et al found a significant correlation

between the location of Delta activity and the lesion location with CT scans and rCBF [19]. Persistent focal Delta activity around lesion was also revealed in patients with brain tumors after surgery [20]. In our studies, the SD imaging of the original MEG around the lesion area showed strong activity in the Delta band, while the data far away from the lesion revealed relatively weak activity within Delta band, which is consistent with the conclusion of previous researches.

An issue is that the original 'C' shape looks like circular area in ECoG and MEG images due to, 1) spatial resolution, but mainly 2) some neighbor points presented strong activities that changed the imaging. The analysis on ECoG could not reveal the true 'C' shape of the hole, which provides sound evidence for the surrounding strong activities smearing the lesion shape information to some extent (Fig. 3). Additionally, because of the relatively low spatial resolution of MEG, the MEG imaging could not distinguish the inactivity area in the lesion, and it was masked by the strong activity in the periphery.

At the beginning of the analysis, the famous Gradient method proposed by Cohen was tried to use to locate the lesion [1]. However, the results are not satisfying. The results are ignored here. If every coil contains only the local information then the gradient should reflect the center between two coils. The neural activity is a stochastic process, according to the Gaussian Central Limit Theorem, the distribution of the sum of the two stochastic processes will converge toward the normal distribution. In particular, there are so many random sources firing simultaneously in the cortex. The real cortex in our study is far less-than-ideal model. It might be the reason why the results of the Gradient method are not satisfying here.

In conclusion, it demonstrates that the first PC represents background activity, and PCA decomposition can be employed to remove it in order to expose the local activity. It is expected to be applied to research on the mapping of lesion area of brain injury, and inactivity area of brain disease, such like Cerebral Palsy, Cerebral Infarct, and Aphasia.

## Acknowledgments

The research was supported by the NIH grants (J. Stephen and T. Zhang - P20AA017068, NCRR P20RR021938, NIGMS P20GM103472), and Natural Science Foundation of Shaanxi Province in China(2014JQ8314).

## References

1. Cohen D, Palti Y, Cuffin BN, Schmid SJ. Magnetic Fields Produced by Steady Currents in the Body. *Proc Natl Acad Sci.* 1980; 77:1447–1451. [PubMed: 6929495]
2. Blanco S, Garcia H, Quiroga QR, Romanelli L, Rosso OA. Stationarity of the EEG Series. *IEEE Eng Med Biol Mag.* 1995; 14:395–399.
3. Kuriki S, Takeuchi F, Kobayashi T. Characteristics of the background fields in multichannel-recorded magnetic field responses. *Electroenceph Clin Neurophysiol.* 1994; 92:56–63. [PubMed: 7508853]
4. Sekihara K, Ogura Y, Hotta M. Maximum-likelihood estimation of current-dipole parameters for data obtained using multichannel magnetometer. *IEEE Trans Biomed Eng.* 1992; 39:558–562. [PubMed: 1601436]
5. Sekihara K, Takeuchi F, Kuriki S, Koizumi H. Reduction of brain noise influence in evoked neuromagnetic source localization using noise spatial correlation. *Phys Med Biol.* 1994; 39:937–946. [PubMed: 15551571]

6. Okada, YC.; Xu, CB. Oscillatory Event-Related Brain Dynamics. Plenum; New York: 1994. Detection of Unaveraged Spontaneous and Event Related Electrophysiological Activities from Focal Regions of the Cerebral Cortex in the Swine.
7. Lagerlund TD, Sharbrough FW, Busacker NE. Spatial filtering of multichannel electroencephalographic recordings through Principal Component Analysis by Singular Value Decomposition. *Journal of Clinical Neurophysiology*. 1997; 14:73–82. [PubMed: 9013362]
8. Kobayashi T, Kuriki S. Principal Component Elimination Method for the Improvement of S/N in Evoked Neuro-magnetic Field Measurements. *IEEE Biomed Eng*. 1999; 46:951–958.
9. Ikeda H, Leyba L, Anton B, Wang Y, Okada YC. Synchronized spikes of thalamocortical axonal terminals and cortical neurons are detectable outside the pig brain with MEG. *Journal of Neurophysiology*. 2002; 87:626–630. [PubMed: 11784777]
10. Okada YC, Lahteenmaki A, Xu C. Comparison of MEG and EEG on the basis of somatic evoked responses elicited by stimulation of the snout in the juvenile swine. *Clinical Neurophysiology*. 1999; 110:214–229. [PubMed: 10210611]
11. Okada YC, Lahteenmaki A, Xu C. Experimental analysis of distortion of magnetoencephalography signals by the skull. *Clinical Neurophysiology*. 1999b; 110:230–238. [PubMed: 10210612]
12. Crone NE, Sinai A, Korzeniewska A. High-frequency gamma oscillations and human brain mapping with electrocorticography. *Event-related Dynamics of Brain Oscillations*. 2006; 159:275–295.
13. Spironelli C, Angrilli A. EEG delta band as a marker of brain damage in aphasic patients after recovery of language. *Neuropsychologia*. 2009; 47:988–994. [PubMed: 19027029]
14. Babiloni C, Frisoni G, Steriade M, Bresciani L, Binetti G, Del Percio C, Geroldi C, Miniussi C, Nobili F, Rodriguez G, Zappasodi F, Carfagna T, Rossini PM. Frontal white matter volume and delta EEG sources negatively correlate in awake subjects with mild cognitive impairment and Alzheimer's disease. *Clinical Neurophysiology*. 2006; 117:1113–1129. [PubMed: 16564740]
15. Penolazzi B, Spironelli C, Angrilli A. Delta EEG activity as a marker of dysfunctional linguistic processing in developmental dyslexia. *Psychophysiology*. 2008; 45:1025–1033. [PubMed: 18803600]
16. Srinivasan R, Russell DP, Edelman GM, Tononi G. Frequency tagging competing stimuli in binocular rivalry reveals increased synchronization of neuromagnetic responses during conscious perception. *J Neurosci*. 1999; 19:5435–5448. [PubMed: 10377353]
17. Winter WR, Nunez PL, Ding J, Srinivasan R. Comparison of the effect of volume conduction on EEG coherence with the effect of field spread on MEG Coherence. *Stat Med*. 2007; 26:3946–3957. [PubMed: 17607723]
18. Malmivuo, J.; Plonsey, R. *Bioelectromagnetism*. Oxford University Press; New York: 1995.
19. Nagata K, Mizukami M, Araki G, Kawase T, Hirano M. Topographic electroencephalographic study of cerebral infarction using computer mapping of the EEG. *Journal of Cerebral Blood Flow and Metabolism*. 1982; 2:79–88. [PubMed: 7061605]
20. De Jongh A, Baayen J, de Munck J, Heethaar R, Vandertop WP, Stam CJ. The influence of brain tumor treatment on pathological delta activity in MEG. *Neuroimage*. 2003; 20:2291–2301. [PubMed: 14683730]

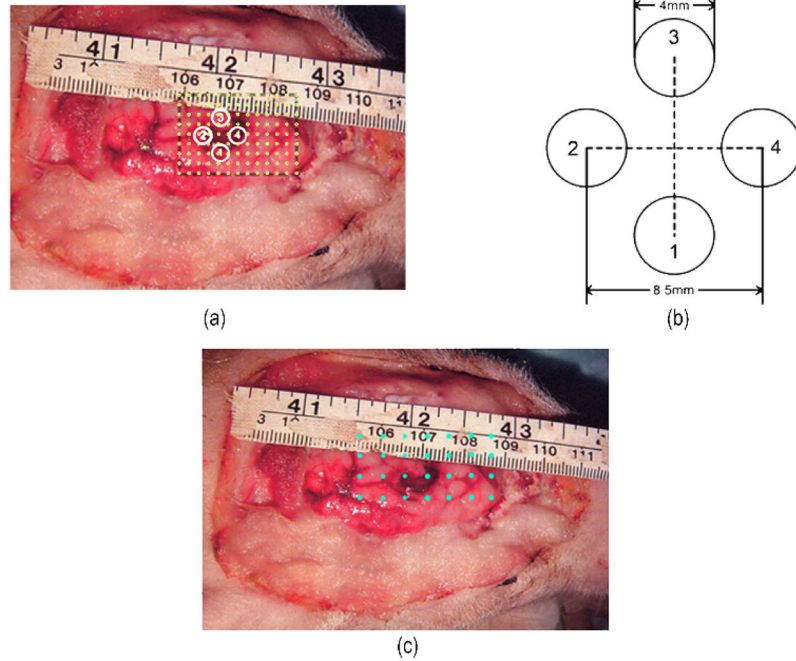


**Fig. 1.**

Animal experiment. (a) Primary somatosensory (SI) cortex of the right hemisphere of a piglet was exposed, and a ‘C’ shape lesion was ablated and filled with agar. The black dash frame depicts the scan area, while the number 1, 2, 3 and 4 represent the 4  $\mu$ SQUID coils at one scan location. Note that here the scan area corresponds to the geometric center of the two-pair of orthogonal coils. The array of 4 coils was shifted by 2 mm along the x and y axes in recording plane of about 18 mm by 26 mm with light dots indicating recording sites. (b) Schematic diagram of the 4-coil configuration. The coils were 4 mm in diameter, separated by 8.5 mm diagonally and arranged orthogonally. (c) Light dots indicate 28 ECoG recording electrodes positioned relative to the neocortex. The Ag/AgCl electrodes were made from silver wire with a diameter of 125  $\mu$ m with 50  $\mu$ m Teflon coating. The wires were interleaved with a nylon mesh sheet which kept the electrodes 5 mm apart along x and y axes.

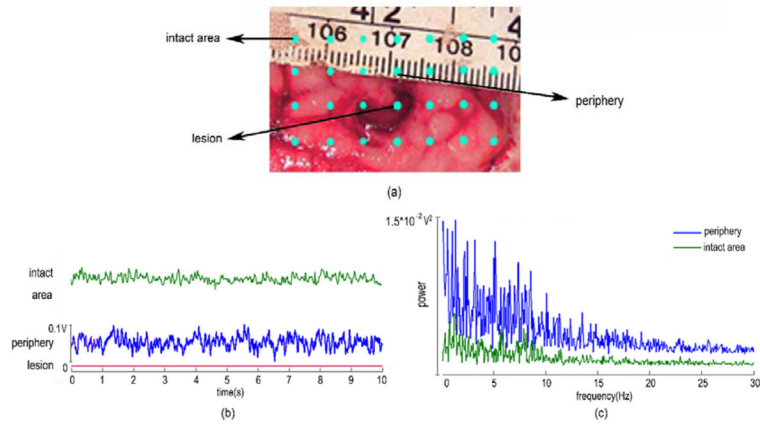


**Fig. 2.** 10 seconds recordings of ECoG signals at 3 locations of a piglet, i.e., lesion, the periphery of the lesion, and the intact area, and their amplitude-frequency spectrum. (a) The selected electrodes at the lesion, the periphery, and the intact area; (b) The signals in time domain; (c) Their corresponding frequency spectrum. Note that the spectrum at lesion that was filled with agar was ignored in (c) due to zeros in (b). The signal at the lesion border presented strong Delta (0.1~5 Hz) activity, and also Theta (5~8 Hz) and Alpha (8~13 Hz) activity.

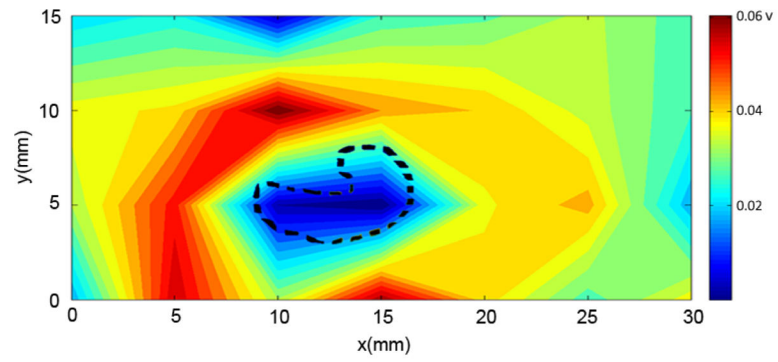


**Fig. 3.**

The image of SD value calculated from the ECoG recordings. The lesion area is in dashed line. Note that the measurement scope of ECoG was not completely the same as MEG. The activity in the lesion was weak, whereas the activity in the periphery was strong compared with the background.

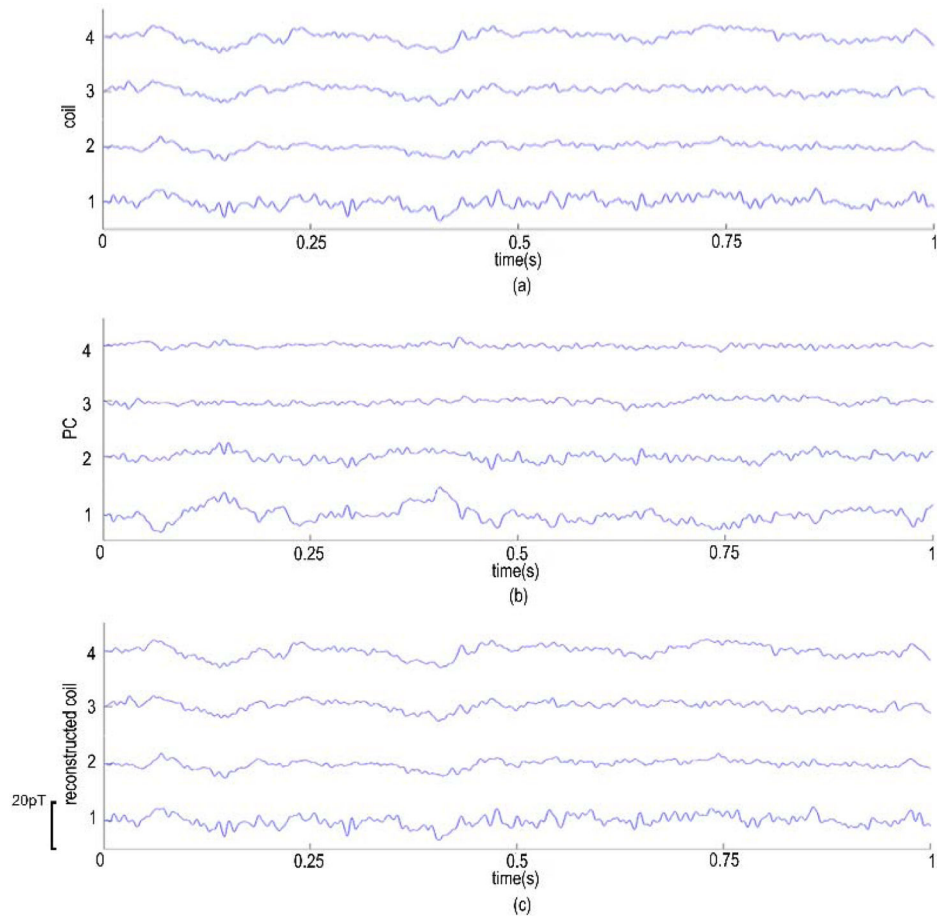


**Fig. 4.**

A typical 1 second spontaneous recording of MEG and the PCA decomposition of a piglet. (a) The spontaneous MEG signals (offline filtered to 0.1–100Hz) recorded by our  $\mu$ SQUID system over neocortex SI area of a piglet; (b) Four PCs after PCA decomposition show that the first PC grabs the prominent common activity in the background; (c) The first PC was projected back to the sensor space to show the common activity in the background. It was multiplied by SD after PCA preprocessing. Note that although channel 1 suffered from higher noise, it still captured the same background activity pattern as the other 3 channels.

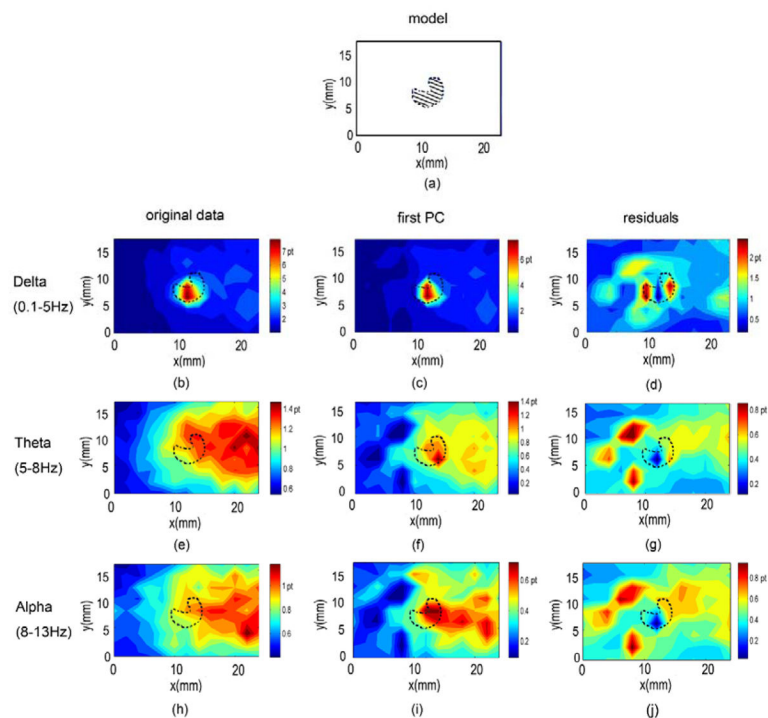


**Fig. 5.**

(a) SD value imaging model of Channel 2. SD value imaging of a piglet calculated from the MEG recordings in Delta, Theta, and Alpha frequency band of Channel 2 for original data ((b), (e) and (h)), first PC ((c), (f) and (i)), and residuals ((d), (g) and (j)) after removing first PC. The lesion location seen by the coil is in dashed line. The images by other channels were similar, but are not shown here. Note that the image is in the sensor coordinate system.

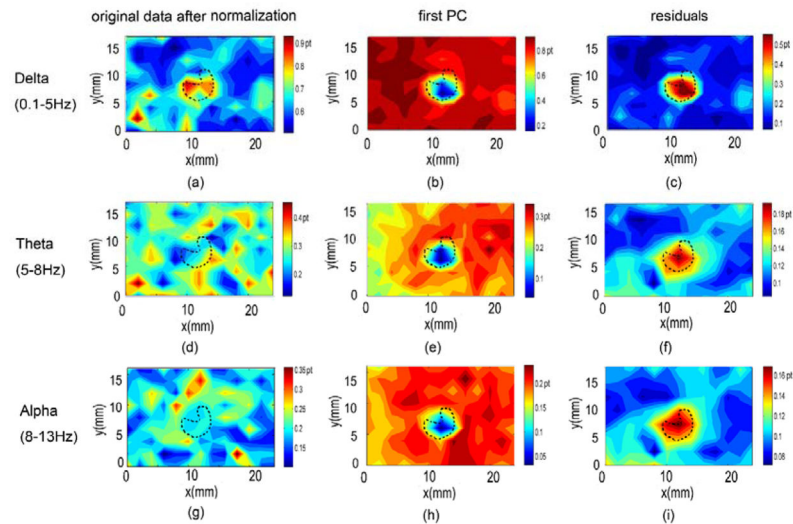


**Fig. 6.**

The images of SD value calculated from the MEG recordings by coil 2 after normalization in Delta, Theta, and Alpha frequency band for original data ((a), (d) and (g)), first PC ((b), (e) and (h)), and residuals ((c), (f) and (i)) after removing first PC. The lesion area seen by the coil is in dashed line. A clear lesion opening, although not exactly the same shape as the lesion, can be seen in (b), (e) and (h), while a strong activity can be seen in the lesion region in (c), (f) and (i). Note that the activity in the lesion periphery was too strong and actually masked the lesion.

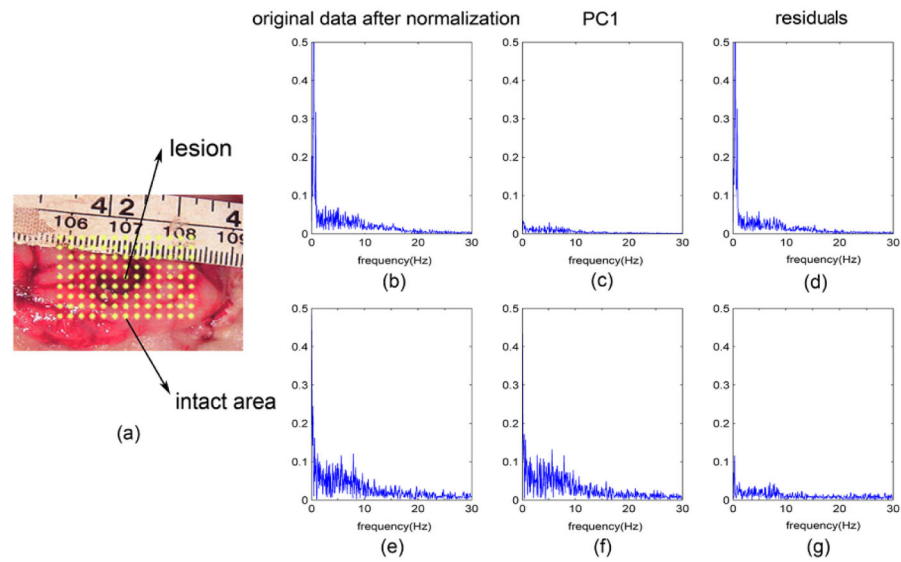
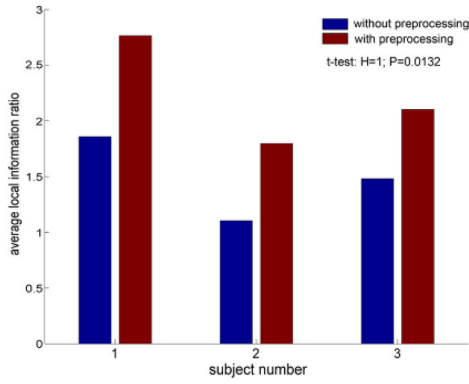
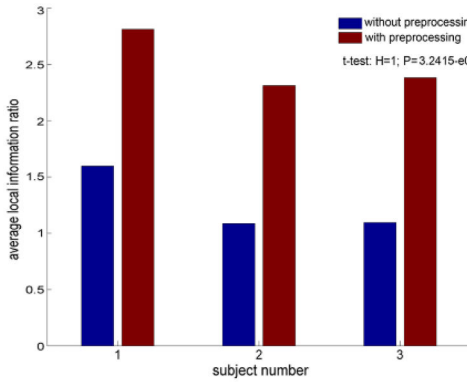


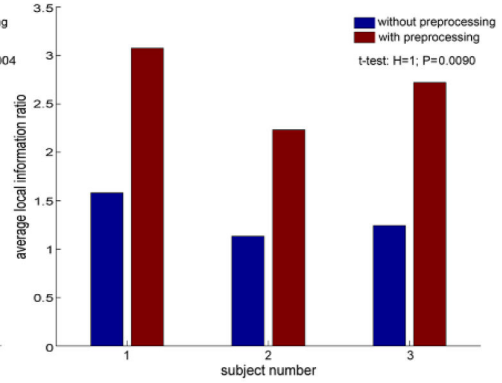
**Fig. 7.** The frequency spectrum of the MEG recordings by Channel 2 in the lesion and intact area, respectively, for original data after normalization, first PC, and residuals after removing first PC. (a) The location of the selected MEG signals at the lesion and intact area; (b)–(d) The frequency spectrum of the MEG in the lesion for the original data after normalization, first PC and residuals; (e)–(g) The frequency spectrum of the MEG in the intact area for the original data after normalization, first PC and residuals.



(a) Delta band (0.1-5 Hz)



(b) Theta band (5-8 Hz)



(c) Alpha band (8-13 Hz)

**Fig. 8.** Average local information ratio over four channels with and without normalized PCA preprocessing in (a) Delta (0.1–5 Hz), (b) Theta (5–8 Hz) and (c) Alpha (8–13 Hz) of three piglets in our study. The average ratio without preprocessing is shown as blue bar, while the ratio with preprocessing as red bar. H and P are the t-test results on average local information ratio with and without normalized PCA preprocessing. A null hypothesis is that the average local information ratio with and without preprocessing comes from distribution with equal means.  $H=0$  indicates the null hypothesis cannot be rejected at the 5% significance level, while  $H=1$  demonstrates it can be rejected at 5% level. P value is the probability if the null hypothesis is true.